JOURNAL OF THEORETICAL AND APPLIED MECHANICS
47, 3, pp. 537-551, Warsaw 2009

APPLICATION OF THE MULTISCALE FEM TO THE MODELING OF NONLINEAR MULTIPHASE MATERIALS

Sandra Ilic
Klaus Hackl

Ruhr-University of Bochum, Institute of Mechanics, Germany
e-mail: sandra.ilic@rub.de; klaus.hackl@rub.de

This contribution is concerned with the modeling of composite materials and, particularly, with the application of the multiscale finite element method for that purpose. The method is a result of combining homogenization theory with the finite element method and is based on the idea of splitting the simulation of a heterogeneous body into two tasks: the first one is the modeling of the actual body and the second one the modeling of the representative volume element, the material sample whose analysis replaces the missing effective constitutive law. The connection of these two simulation levels is achieved by introducing the Hill macrohomogeneity condition which requires the equality of the macropower and the volume average of the micropower. The method has the advantage to be applicable for simulation of materials with very different microstructure types. This is illustrated by the examples concerned with effective behavior of two- and three-phase composite materials.

Key words: multiscale FEM, composite materials, homogenization

1. Introduction

The modeling of composite materials has already a long history. It starts with the well known solutions of Voigt (1889) and Reuss (1929) which are even today often used because of their simplicity. These solutions are pretty intuitive: Voigt's approach states that the effective material tensor is just a volume average of the elasticity tensor of the original composite while the Reuss solution claims the same but for the compliance tensor. A further fundamental contribution to this field has been made by Hill (1952, 1963, 1972). Among others, he introduced the idea of energy bounds and shown that the solutions of Voigt and Reuss can be obtained from the upper and lower energy bounds for the

assumed homogeneous state of strain and stress. Hill's work opened many new possibilities for the modeling of composite materials, with a tendency to find the narrowest possible energy bounds. This idea was also followed in the works of Hashin and Shtrikman (1962a,b, 1963), proposing energy bounds based on the consideration of a comparison homogeneous body. Such an approach was also suggested in contributions considering the modeling of nonlinear composite materials (Castañeda, 1991, 1992; Talbot and Willis, 1985).

Finally, the complexity of analytical solutions as well as the rush development of computer technology gave rise to the strong development of numerical methods appropriate for the modeling of composites. Some methods which are currently used most frequently are those of domain decomposition, adaptive hierarchical modeling and the multiscale FEM.

The essential idea of the domain decomposition method (Zohdi and Wriggers, 1999; Zohdi *et al.*, 2001) is to choose a homogeneous substitute material used to calculate the approximative deformation of the whole body, the so-called regularized problem. Furthermore, the body is decomposed into several subdomains where the real material structure is considered. The boundary conditions at this level are the deformations calculated in the regularized step. The final result is obtained as a superposition of the regularized solution (step I) and local perturbations of the regularized solution for each particular subdomain (step II). From the aspect of numerical costs, the method is very convenient as a big system of equations is split into several small ones.

The method of hierarchical adaptivity (Oden and Zohdi, 1997; Zohdi *et al.*, 1993) also starts from the idea of regularization. Here again a substitute material, not necessarily homogeneous, is chosen. The domain is decomposed in several partitions, in each of them the error due to the regularization is calculated and compared with a prescribed tolerance. For the subdomains where the error bound is exceeded, a new finer subpartitioning is carried out and more precise data on the material microstructure are introduced. The process is iteratively continued until the error remains in the permitted domain for all subpartitions.

A basic disadvantage of both numerical methods mentioned is that in spite of the even high-level partitioning, the influences of the very fine microstructure cannot be caught. This disadvantage is eliminated in the approaches belonging to the group of homogenization methods which has been developed for the so-called statistically uniform materials. This kind of materials has a crucial property that a corresponding representative volume element (RVE) can be defined for them. An RVE represents the smallest material sample containing enough information about the material microstructure such that the

analysis of it yields the same effective material parameters independent from its shape. The notion of the RVE is rather important as the application of the homogenization concept assumes that the ratio of the characteristic size of the RVE and of the simulated body has to tend to zero. The multiscale finite element method (Hackl and Ilic, 2005; Ilic, 2008; Ilic and Hackl, 2004, 2005, 2006; Miehe *et al.*, 2002a,b,c; Schröder, 2000), which is the main topic of this contribution, also belongs to the group of homogenization methods, and its concept and application within the paper will be presented as follows.

The basic definitions and theorems of the homogenization theory are explained in Section 2. The combination of this method with the finite element method (FEM) is demonstrated on a particular example concerned with the nonlinear elastic materials with the potential proposed by Simo, Taylor and Pister (Chap. 3). In Section 4, we consider two numerical examples. The first example investigates the effective material parameters of a material with circular microinclusions periodically ordered in the matrix material. The second example intends to simulate materials with the transit region around the inclusion representing a mixture of the matrix and inclusion material. The paper ends with several conclusions and a brief outlook.

2. Homogenization theory

As indicated in the introduction, the concept of homogenization requires two problems to be simultaneously studied: the modeling of the macroscopic body and the analysis of an RVE corresponding to its material structure. Of course, the quantities related to different problems are dependent on each other. Moreover, according to Hill (1972), the macroscopic quantities are dependent only on the microquantities occurring at the boundary of the RVE. This can be easily explained if the RVE is understood as a small piece cut from the macroscopic body. Then the influences of the body on the cut part are just those occurring at the boundary of the RVE and not those inside it. Another motivation is provided by the fact that laboratory investigations are carried out on the boundary of the sample, being an RVE in the present case.

As we are particularly interested in the theory of finite deformations, the definitions of the macroscopic first Piola-Kirchhoff stress tensor $\overline{\mathbf{P}}$ and deformation gradient $\overline{\mathbf{F}}$ will be elucidated especially in the following. Note that hereafter the overbar symbol will be used to denote the quantities related to the macrolevel while those without overbar symbol relate to the microlevel. For the definition of the macroscopic quantities, an arbitrary RVE $\mathcal{B}$ with the

boundary $\partial\mathcal{B}$ is considered (Fig. 1). Such an RVE may also contain one or more voids and their boundaries are denoted by $\mathcal{G}$ in Fig. 1. It is also possible to study the singular surfaces inside the RVE, but in that case mostly the zero jump of the deformations is assumed which leads to the same definitions as they are presented here (Schröder, 2000).

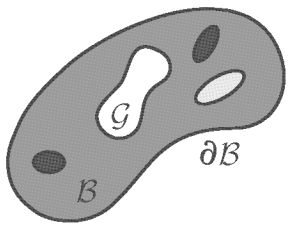

Fig. 1. An arbitrary RVE with a cavity

In order to define the first Piola-Kirchhoff macrostress tensor, the analysis is started by observing that the volume average of its microscopic counterpart over the volume V of the RVE $\mathcal{B}$ is

$$\langle \mathbf{P} \rangle = \frac{1}{V} \int_{\mathcal{B}} \mathbf{P} \, dV \tag{2.1}$$

Here the volume average is denoted by the symbol $\langle \cdot \rangle$. Bearing in mind that $\mathbf{P} = \mathbf{0}$ on the boundary parts without load (such as the boundaries of the intrinsic voids $\mathcal{G}$) and that Grad $\boldsymbol{X} = \mathbf{I}$, Eq. (2.1) can be transformed into the following boundary integral

$$\frac{1}{V} \int_{\mathcal{B}} \mathbf{P} \, dV = \frac{1}{V} \int_{\partial\mathcal{B}} (\mathbf{P}\boldsymbol{N}) \otimes \boldsymbol{X} \, dA = \frac{1}{V} \int_{\partial\mathcal{B}} \boldsymbol{T} \otimes \boldsymbol{X} \, dA \tag{2.2}$$

Here $\boldsymbol{T}$ represents the tractions, i.e. it holds $\boldsymbol{T} = \mathbf{P}\boldsymbol{N}$, $\boldsymbol{X}$ is the position vector and $\boldsymbol{N}$ the normal vector on the surface of the boundary, all of them in the reference configuration. The notation " Grad " represents differentiation with respect to the coordinates in the reference coordinate system. As the volume average of the microscopic stress tensor can be rewritten as an expression depending only on quantities occurring at the boundary of the RVE (2.2), the volume average can be directly assumed as the definition of the macroscopic Piola-Kirchhoff stress tensor

$$\overline{\mathbf{P}} = \langle \mathbf{P} \rangle = \frac{1}{V} \int_{\mathcal{B}} \mathbf{P} \, dV \tag{2.3}$$

A similar procedure repeated for the microdeformation gradient yields its volume average in the form

$$\frac{1}{V}\int\limits_{\mathcal{B}} \mathbf{F}\, dV = \frac{1}{V}\Big(\int\limits_{\partial\mathcal{B}} \boldsymbol{x}\otimes\boldsymbol{N}\, dA + \int\limits_{\mathcal{G}} \boldsymbol{x}\otimes\boldsymbol{N}\, dA\Big) \tag{2.4}$$

where $\boldsymbol{x}$, in contrast to $\boldsymbol{X}$, denotes the coordinates in the current configuration. Obviously, the volume average cannot be expressed dependent only on a single boundary integral over the external boundary of the RVE as the deformations at the internal boundaries are, in general, different from zero. For this reason we take the first term at the right hand side of (2.4) as the definition of the macrodeformation tensor

$$\overline{\mathbf{F}} := \frac{1}{V}\int\limits_{\partial\mathcal{B}} \boldsymbol{x}\otimes\boldsymbol{N}\, dA = \frac{1}{V}\Big(\int\limits_{\mathcal{B}} \mathbf{F}\, dV - \int\limits_{\mathcal{G}} \boldsymbol{x}\otimes\boldsymbol{N}\, dA\Big) \tag{2.5}$$

Obviously, in the case of the continuous composite materials, the macrodeformation tensor can be equalized with the volume average of its microscopic counterpart.

Given the definitions of the macroscopic quantities, the last component that needs to be specified are the boundary conditions at the microlevel. To this end, an additional requirement concerning the connection of macro and micro power is introduced. This is known as the Hill condition and states that macropower must be equal to the volume average of the micropower (Hill, 1963, 1972; Huet, 1990)

$$\overline{\mathbf{P}} : \dot{\overline{\mathbf{F}}} = \frac{1}{V}\int\limits_{\mathcal{B}} \mathbf{P} : \dot{\mathbf{F}}\, dV \tag{2.6}$$

An alternative form of the Hill condition (2.6) can be derived by means of the Gauss theorem

$$\frac{1}{V}\int\limits_{\partial\mathcal{B}} (\boldsymbol{T} - \overline{\mathbf{P}}\boldsymbol{N})(\dot{\boldsymbol{x}} - \dot{\overline{\mathbf{F}}}\boldsymbol{X})\, dA = 0 \tag{2.7}$$

This expression is especially convenient as it allows one to directly define two types of boundary conditions satisfying (2.6) and (2.7), respectively. These conditions are known as the static boundary conditions

$$\boldsymbol{T} = \mathbf{P}\boldsymbol{N} \qquad \text{on } \partial\mathcal{B} \tag{2.8}$$

and the kinematic boundary conditions

$$\boldsymbol{x} = \overline{\mathbf{F}}\boldsymbol{X} \qquad \text{on } \partial\mathcal{B} \tag{2.9}$$

and because of their simplicity they are regularly applied in laboratory investigations. A further possible solution to (2.7) is derived by using the assumption that the real deformation at the microscale is equal to the macrodeformation superimposed with microfluctuations $\widetilde{\boldsymbol{w}}$

$$\boldsymbol{x} = \overline{\mathbf{F}}\boldsymbol{X} + \widetilde{\boldsymbol{w}} \tag{2.10}$$

Substitution of this assumption into (2.7) results in the conclusion that this condition is also satisfied in the case that the microfluctuations $\widetilde{\boldsymbol{w}}$ are periodic and the tractions $\boldsymbol{T}$ antiperiodic at the periodic boundary of the RVE

$$\widetilde{\boldsymbol{w}}^{+} = \widetilde{\boldsymbol{w}}^{-} \qquad \boldsymbol{T}^{+} = -\boldsymbol{T}^{-} \tag{2.11}$$

Here the superscripts "+" and "−" distinguish the quantities related to the boundary parts whose normal vectors are oppositely oriented: $\boldsymbol{N}^{+} = -\boldsymbol{N}^{-}$. The investigations show that this type of boundary conditions leads to very good results even if the microstructure is not perfectly periodic (Zohdi and Wriggers, 2005). An important advantage of using assumption (2.10) is the simple relation of the microdeformation tensor: it is just a superposition of the macrodeformation and the microfluctuation gradient

$$\mathbf{F} = \operatorname{Grad}\boldsymbol{x} = \overline{\mathbf{F}} + \operatorname{Grad}\widetilde{\boldsymbol{w}} = \overline{\mathbf{F}} + \widetilde{\mathbf{F}} \tag{2.12}$$

3. FEM implementation

Let us summarize the data of the boundary value problems (BVPs) that are to be solved within the scope of homogenization theory. The first BVP is concerned with the simulation of the macroscopic body. Here the geometry as well as the loads are defined. The material properties and the material tensor or directly the stress tensors are obtained from the microscale calculations. The second BVP considers the behavior of the RVE for the macrodeformation obtained as the input from the macroscale, and the periodic (alternatively static or kinematic) boundary conditions derived from the Hill condition have to be satisfied. The geometry including the material characteristics at this level is known. Obviously, after introducing the Hill macrohomogeneity condition, both BVPs are complete and any standard method can be used for their solution. Our particular choice considers a combination of homogenization theory with FEM, known as the multiscale or FE^2 method. The advantage of this approach is that it is easily adaptable for simulating materials with very

different microstructures. This applies to the geometry of the RVE as well as to the constitutive laws of the component materials.

Within this contribution we will consider a case where the material behavior at both scales is determined by the following potential in the three-field description (Simo and Hughes, 1997)

$$\Pi(\boldsymbol{u},\Theta,p)=\int_V[\Psi_{vol}(\Theta)+\Psi_{dev}(\mathbf{C}^*(\boldsymbol{u}))+p(J(\boldsymbol{u})-\Theta)]\,dV+\Pi^{ext} \tag{3.1}$$

Its advantage in comparison with the standard formulation is the applicability to cases of nearly incompressible materials. This is achieved by introducing the secondary variables Θ and p, permitting the potential to be split into a deviatoric and a volumetric part. The new variables Θ and p represent the volumetric change and hydrostatic pressure respectively, $\mathbf{C}^*$ is the isochoric right Cauchy Green deformation tensor defined as $\mathbf{C}^*=J^{-\frac{2}{3}}\mathbf{C}$, and $J=\det\mathbf{F}$ is the Jacobian. For a complete specification of the material behavior, the Helmholtz free energy corresponding to the Neo-Hook material is chosen

$$\Psi=\Psi_{dev}+\Psi_{vol}=\frac{1}{2}\mu(\operatorname{tr}\overline{\mathbf{C}}-3)+K(J\ln J-J+1) \tag{3.2}$$

where K and μ are the bulk and shear moduli, respectively.

Since the potential is fixed, we can now focus on the FEM implementation. To this end the second variation of (3.1) is needed, and using the standard tools of variational calculus (Boonet and Wood, 2000; Simo and Hughes, 1997) it can be shown that the necessary expression has the form

$$\begin{aligned}
&\int_{\overline{V}}\overline{\operatorname{Grad}}\,\delta\overline{\boldsymbol{u}}:[\overline{\operatorname{Grad}}\,\Delta\overline{\boldsymbol{u}}\cdot(\overline{\mathbf{S}}_{dev}+\overline{\mathbf{S}}_{vol})]\,d\overline{V}+\\
&\quad+\int_{\overline{V}}(\overline{\operatorname{Grad}}^{\top}\delta\overline{\boldsymbol{u}}\cdot\overline{\mathbf{F}}):(\overline{\mathbf{A}}_{dev}+\overline{\mathbf{A}}_{vol}):(\overline{\mathbf{F}}^{\top}\cdot\overline{\operatorname{Grad}}\,\Delta\overline{\boldsymbol{u}})\,d\overline{V}+\\
&\quad+\int_{\overline{V}}(\overline{\operatorname{Grad}}^{\top}\delta\overline{\boldsymbol{u}}\cdot\overline{\mathbf{F}}):\overline{J}\,\overline{\mathbf{C}}^{-1}d\overline{V}\Big(\frac{1}{\overline{V}}\frac{\partial^2\overline{\Psi}_{vol}}{\partial\overline{\Theta}^2}\Big)\int_{\overline{V}}\overline{J}\,\overline{\mathbf{C}}^{-1}:(\overline{\mathbf{F}}^{\top}\cdot\overline{\operatorname{Grad}}\,\Delta\overline{\boldsymbol{u}})d\overline{V}+\\
&\quad+\Delta\delta_{\overline{\boldsymbol{u}}}\overline{\Pi}^{ext}=-\delta_{\overline{\boldsymbol{u}}}\overline{\Pi}^{res}
\end{aligned} \tag{3.3}$$

$$\begin{aligned}
&\overline{\boldsymbol{u}}=\boldsymbol{u}_0,\quad \delta\overline{\boldsymbol{u}}=\mathbf{0},\quad \Delta\overline{\boldsymbol{u}}=\mathbf{0} && \text{on}\quad \partial\overline{\mathcal{B}}_{\overline{u}}\\
&\overline{\boldsymbol{t}}=\overline{\boldsymbol{t}}_0 && \text{on}\quad \partial\overline{\mathcal{B}}_{t}
\end{aligned}$$

Recall that the second variation in this concept represents the linearized form of the condition that the actual state of the deformation minimizes the potential. In (3.3), the following notation is used: Δ denotes the increment, $\overline{\mathbf{S}}_{dev}$ and

$\overline{\mathbf{S}}_{vol}$ are the deviatoric and volumetric parts of the second Piola-Kirchhoff stress tensor, defined in a standard way as

$$\overline{\mathbf{S}}_{dev} = 2\frac{\partial \overline{\Psi}_{dev}(\overline{\mathbf{C}})}{\partial \overline{\mathbf{C}}} \qquad \overline{\mathbf{S}}_{vol} = 2\frac{\partial \overline{\Psi}_{vol}(\overline{\mathbf{C}})}{\partial \overline{\mathbf{C}}} \tag{3.4}$$

and $\overline{\mathbf{A}}_{dev}$ and $\overline{\mathbf{A}}_{vol}$ are the corresponding elasticity tensors

$$\begin{aligned} \overline{\mathbf{A}}_{dev} &= 2\frac{\partial \overline{\mathbf{S}}_{dev}}{\partial \overline{\mathbf{C}}} = 4\frac{\partial^2 \overline{\Psi}_{dev}(\overline{\mathbf{C}})}{\partial \overline{\mathbf{C}}^2} \\ \overline{\mathbf{A}}_{vol} &= 2\frac{\partial \overline{\mathbf{S}}_{vol}}{\partial \overline{\mathbf{C}}} = 4\frac{\partial^2 \overline{\Psi}_{vol}(\overline{\mathbf{C}})}{\partial \overline{\mathbf{C}}^2} \end{aligned} \tag{3.5}$$

The derivative of the pressure has to be calculated according to

$$\frac{\partial^2 \overline{\Psi}_{vol}(\overline{\mathbf{C}})}{\partial \overline{\Theta}^2} = \frac{\partial \overline{p}}{\partial \overline{J}} = \frac{2}{3}\overline{J}\frac{\partial \overline{p}}{\partial \overline{\mathbf{C}}} : \overline{\mathbf{C}}^* \tag{3.6}$$

As expression (3.3) exactly corresponds to the BVP at the macroscale, the overbar symbol is directly introduced. The particularity of the macroscale problem is that the quantities dependent on $\overline{\Psi}(\overline{\mathbf{C}})$, such as the stresses and their derivatives, cannot be calculated directly but using the microscale results, expression (2.3) and relation $\overline{\mathbf{S}} = \overline{\mathbf{F}}^{-1}\overline{\mathbf{P}}$. For the calculation of $\overline{\mathbf{A}}_{dev}$, $\overline{\mathbf{A}}_{vol}$ and $\partial\overline{p}/\partial\overline{\mathbf{C}}$, the numerical derivatives must be used in addition.

The same material description (3.1) is used at the microlevel so that for the macrodeformation imposed from the macrolevel (in the calculation it is treated as the value from the previous step of Newton Raphson iteration) and neglecting the external load, the microlevel BVP becomes

$$\begin{aligned} &\int_V \operatorname{Grad}\delta\widetilde{\boldsymbol{w}} : [\operatorname{Grad}\Delta\widetilde{\boldsymbol{w}} \cdot (\mathbf{S}_{dev} + \mathbf{S}_{vol})]\, dV + \\ &\quad + \int_V (\operatorname{Grad}^{\top}\delta\widetilde{\boldsymbol{w}} \cdot \mathbf{F}) : (\mathbf{A}_{dev} + \mathbf{A}_{vol}) : (\mathbf{F}^{\top} \cdot \operatorname{Grad}\Delta\widetilde{\boldsymbol{w}})\, dV + \\ &\quad + \int_V (\operatorname{Grad}^{\top}\delta\widetilde{\boldsymbol{w}} \cdot \mathbf{F}) : J\mathbf{C}^{-1}\, dV \Big(\frac{1}{V}\frac{\partial^2 \Psi_{vol}}{\partial \Theta^2}\Big) \int_V J\mathbf{C}^{-1} : (\mathbf{F}^{\top} \cdot \operatorname{Grad}\Delta\widetilde{\boldsymbol{w}})\, dV + \\ &\quad + \delta_{\widetilde{\boldsymbol{w}}} \Pi^{res}_{mac} = -\delta_{\widetilde{\boldsymbol{w}}} \Pi^{res} \end{aligned} \tag{3.7}$$

$$\widetilde{\boldsymbol{w}}^{+} = \widetilde{\boldsymbol{w}}^{-}, \quad \delta\widetilde{\boldsymbol{w}} = \mathbf{0}, \quad \Delta\widetilde{\boldsymbol{w}} = \mathbf{0} \qquad \text{on } \partial\mathcal{B}$$

$$\delta_{\widetilde{\boldsymbol{w}}} \Pi^{res}_{mac} = f(\overline{\mathbf{F}})$$

In contrast to (3.3), this expression depends on the microfluctuations $\widetilde{\boldsymbol{w}}$. Periodic boundary conditions as a consequence of the Hill macrohomogeneity conditions are assumed. Of course static or kinematic boundary conditions are possible alternatives but due to the periodic microstructure of the materials, which will be simulated here, periodic boundary conditions are chosen.

The further procedure includes the standard steps of FE implementation (Hughes, 1987; Zienkiewicz and Taylor, 2000). To this end, the displacement function and its derivatives are approximated by means of the shape functions and nodal values

$$\begin{aligned} &\overline{\boldsymbol{u}} = \overline{\mathbf{N}}\widehat{\boldsymbol{u}}^e \\ &\overline{\mathrm{Grad}}\,\overline{\boldsymbol{u}} = \overline{\mathbf{B}}\widehat{\boldsymbol{u}}^e \qquad\qquad \overline{\mathbf{B}} = \overline{\mathrm{Grad}\,\mathbf{N}}^e \end{aligned} \tag{3.8}$$

and analogous expressions hold also for the increment and variation of displacements

$$\overline{\mathrm{Grad}}\,\Delta\overline{\boldsymbol{u}} = \overline{\mathbf{B}}\Delta\widehat{\boldsymbol{u}}^e \qquad\qquad \overline{\mathrm{Grad}}\,\delta\overline{\boldsymbol{u}} = \overline{\mathbf{B}}\delta\widehat{\boldsymbol{u}}^e \tag{3.9}$$

Here $\overline{\mathbf{N}}$ is a matrix containing the shape functions and $\overline{\mathbf{B}}$ is a matrix containing the derivatives of the shape functions with respect to the physical coordinates $\overline{\boldsymbol{X}}$. A hat symbol denotes the nodal values and e indicates that all the DOFs of an element are considered. The implementation of (3.8) and (3.9) into (3.7) yields the element stiffness matrix $\overline{\mathbf{K}}^e$

$$\begin{aligned} \overline{\mathbf{K}}^e = &\int_{\overline{V}^e} \overline{\mathbf{G}}^{\top}(\overline{\mathbf{S}}_{dev} + \overline{\mathbf{S}}_{vol})\overline{\mathbf{G}}\; d\overline{V} + \int_{\overline{V}^e} (\overline{\mathbf{B}}^{\top}\overline{\mathbf{F}}) : (\overline{\mathbf{A}}_{dev} + \overline{\mathbf{A}}_{vol}) : (\overline{\mathbf{F}}^{\top}\overline{\mathbf{B}})\; d\overline{V} + \\ &+ \int_{\overline{V}^e} (\overline{\mathbf{B}}^{\top}\overline{\mathbf{F}}) : \overline{J\mathbf{C}}^{-1}\; d\overline{V} \Big(\frac{1}{\overline{V}}\frac{\partial^2 \overline{\Psi}_{vol}}{\partial \overline{\Theta}^2}\Big) \int_{\overline{V}^e} \overline{J\mathbf{C}}^{-1} : (\overline{\mathbf{F}}^{\top}\overline{\mathbf{B}})\; d\overline{V} \end{aligned} \tag{3.10}$$

with matrix $\overline{\mathbf{G}}$ being defined in the following way

$$\begin{aligned} &\int_{\overline{V}^e} \overline{\mathrm{Grad}}\,\delta\overline{\boldsymbol{u}} : [\overline{\mathrm{Grad}}\,\Delta\overline{\boldsymbol{u}} \cdot (\overline{\mathbf{S}}_{dev} + \overline{\mathbf{S}}_{vol})]\; d\overline{V} = \\ &\qquad + \delta\widehat{\boldsymbol{u}} \int_{\overline{V}^e} [\overline{\mathbf{G}}^{\top}(\overline{\mathbf{S}}_{dev} + \overline{\mathbf{S}}_{vol})\overline{\mathbf{G}}]\; d\overline{V}\,\Delta\widehat{\boldsymbol{u}} \end{aligned} \tag{3.11}$$

Of course, an approximation of the fluctuations $\widetilde{\boldsymbol{w}}$ at the microlevel is also required, but this procedure is analogous to steps (3.8)-(3.11) and yields the

same results, so that it will not be repeated. The approximation for macrodeformations $(3.8)_1$ and its microscopic counterpart can be chosen in a different manner dependent on the type of problems to be solved. In the current simulations, the P0Q1 element with bilinear shape functions (Hughes, 1987; Zienkiewicz and Taylor, 2000) is taken at both levels.

4. Numerical examples

Our first example examines materials whose microstructure is determined by a square RVE containing a circular inclusion (Fig. 2). The square has unit side length $2d = 1\,\text{mm}$ and the inclusion of radius $r = 0.125\,\text{mm}$ is placed centrally. The material parameters of the matrix material are fixed: the Young modulus amounts to $1000\,\text{N/mm}^2$ and the Poisson ratio is 0.3. The Young modulus of the inclusions is varied in different tests, and it takes values in the range of 0-1000 N/mm^2. The Poisson ratio of the inclusion is constant: $\nu = 0.3$. The plane strain state is assumed.

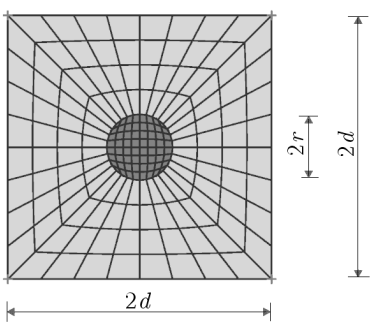

Fig. 2. Microlevel: RVE of two-phase material with circular inclusion

The microstructure being defined, a tension test of a square plate is considered at the macroscale. The plate has the dimensions $40 \times 40\,\text{cm}$, but due to symmetry consideration of one fourth of the plate is satisfactory (Fig. 3). Here, in addition, the vertical displacements at the lower boundary and horizontal displacements at the left boundary must be constrained. The mesh consists of 10×10 elements with four Gauss points, and to each of these points an RVE is associated. The load chosen is $p = 1\,\text{kN/cm}$.

The final results of the tension tests are the displacements of the unconstrained boundaries, further used for calculation of the effective material parameters presented in Fig. 4. Here both diagrams show a smooth increase of

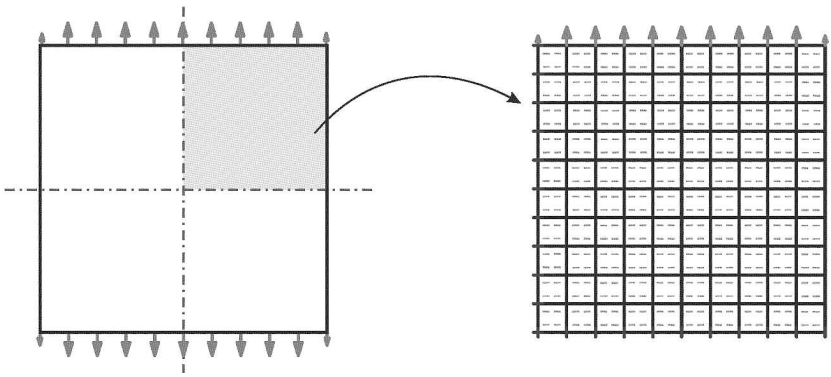

Fig. 3. Macrolevel: Tension test of a plate

the effective material parameters with respect to a change of Young's modulus of the inclusion. The effective Young modulus takes values in the range of 886.7-1000 $\mathrm{N/mm^2}$ and Poisson's ratio 0.29-0.3. Notice that the values obtained for the zero Young's modulus of inclusion $(E_I = 0)$ correspond to microporous material while the other limit case $(E_I = 1000\,\mathrm{N/mm^2})$ corresponds to the homogeneous material as the matrix and the inclusion have the same properties.

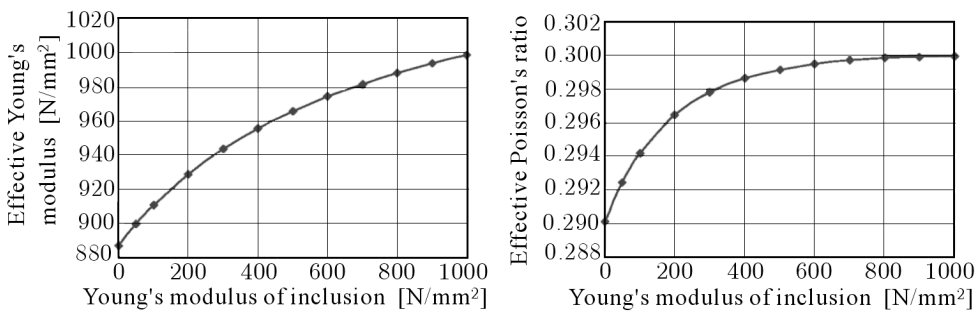

Fig. 4. Change of Young's modulus and Poisson's ratio with respect to Young's modulus of the inclusion. Two-phase material is considered

The second example studies a more complex geometry. The RVE is still a unit square with a circular inclusion of radius 0.125 mm, but a third phase is introduced in addition (Fig. 5). This phase forms a ring with the internal radius $r = 0.125$ mm and external radius $r = 0.25$ mm. The intention here is to simulate a belt consisting of a mixture of the matrix and inclusion material. Accordingly, the Young modulus of the third phase takes values in the range of 300-1000 $\mathrm{N/mm^2}$, where the first value is typical for the inclusion and the

second one for the matrix material. The former limit case corresponds to the two-phase material with an inclusion of radius 0.25 mm and the later limit case to the two-phase material with the inclusion of radius 0.125 mm (as in the previous example). The macroscale problem remains unchanged: a tension test of the plate results in displacements used for calculation of the effective material parameters (Fig. 3). The values calculated for the new type of microstructure are presented in Fig. 6. Here, again, both diagrams show a smooth, gradual increase of the effective parameters.

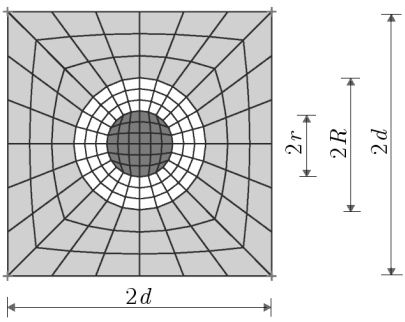

Fig. 5. Microlevel: RVE of a three-phase material with a circular inclusion and mixture belt

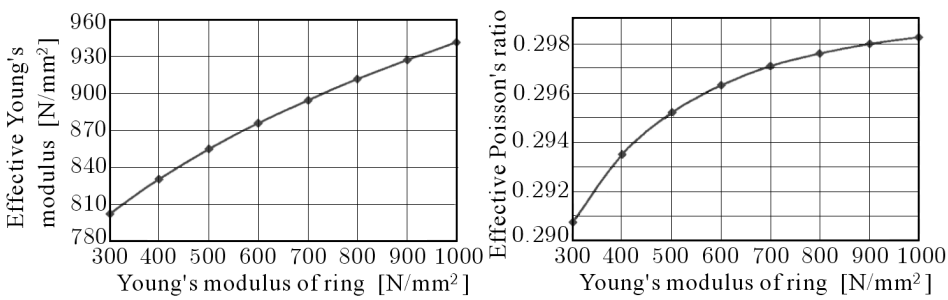

Fig. 6. Change of Young's modulus and Poisson's ratio with respect to Young's modulus of the ring. Three-phase material is considered

5. Conclusions

The present contribution is focused on an approach to the modeling of composites known as the multiscale FEM. In order to demonstrate the concept and implementation of this method, we chose a particular material with the potential in three-field description and the free Helmholtz energy corresponding to

the Neo-Hook material. For such a combination, two illustrative examples are considered. The first shows the change of the effective material parameters in the case of a material with periodic microstructure with a circular inclusion whereby the material parameters of the inclusion are varied. The second example also considers the periodic microstructure with a circular inclusion, but in addition a narrow belt around this inclusion is introduced. In this test group, Young's modulus of the belt varies taking values from the range limited by the values characteristic for the inclusion and matrix material. The resulting diagrams for both examples show a gradual increase of the effective material parameters.

The simulations presented endorse that the multiscale FEM can be reliably applied to the modeling of composite materials with complex microstructure. This is a strong motivation for further concentrating on the modeling of practice-oriented macro- and microscale problems such as estimation of the effective properties of damaged materials or simulation of composites consisting of solid and fluid fractions, which is typical for biomechanics. The 3D simulations as well as the implementation of the static and kinematic boundary conditions at the microlevel are some other challenging topics to be investigated.

References

1. Boonet J., Wood R.D., 2000, *Nonlinear Continuum Mechanics for Finite Element Analysis*, Cambridge University Press

2. Castañeda P.P., 1991, The effective mechanical properties of nonlinear isotropic composites, *J. Mech. Phys. Solids.*, **39**, 1, 45-71

3. Castañeda P.P., 1992, New variational principles in plasticity and their application to composite materials, *J. Mech. Phys. Solids.*, **40**, 8, 1757-1788

4. Hackl K. Ilic S., 2005, Solution-precipitation creep – continuum mechanical formulation and micromechanical modelling, *Arch. Appl. Mech.*, **74**, 773-779

5. Hashin Z., Shtrikman S., 1962a, A variational approach to the theory of the elastic behaviour of polycrystals, *J. Mech. Phys. Solids*, **10**, 343-352

6. Hashin Z., Shtrikman S., 1962b, On some variational principles in anisotropic and nonhomogeneous elasticity, *J. Mech. Phys. Solids*, **10**, 335-342

7. Hashin Z., Shtrikman S., 1963, A variational approach to the theory of the elastic behaviour of multiphase materials, *J. Mech. Phys. Solids*, **11**, 127-140

8. Hill R., 1952, The elastic behaviour of a crystalline aggregate, *Proc. Phys. Soc., London, A*, **65**, 349-354

9. Hill R., 1963, Elastic properties of reinforced solids: some theoretical principles, *J. Mech. Phys. Solids*, **11**, 357-372

10. Hill R., 1972, On constitutive macro-variables for heterogeneous solids at finite strain, *Proc. R. Soc. Lond., A*, **326**, 131-147

11. Huet C., 1990, Application of variational concepts to size effects in elastic heterogeneous bodies, *J. Mech. Phys. Solids*, **38**, 6, 813-841

12. Hughes T.J.R., 1987, *The Finite Element Method*, Prentice Hall, Englewood Cliffs, NJ

13. Ilic S., 2008, *Application of the Multiscale FEM to the Modeling of Composite Materials*, Ph.D. Thesis, Ruhr-University Bochum

14. Ilic S., Hackl K., 2004, Homogenisation of random composites via the multiscale finite-element method, *PAMM*, **4**, 326-327

15. Ilic S., Hackl K., 2005, Solution-precipitation creep – micromechanical modelling and numerical results, *PAMM*, **5**, 277-278

16. Ilic S., Hackl K., 2006, Multiscale FEM in modelling of solution-precipitation creep, *PAMM*, **6**, 483-484

17. Miehe C., Schotte J., Lambrecht M., 2002a, Homogenisation of inelastic solid materials at finite strains based on incremental minimization principles, *J. Mech. Phys. Solids*, **50**, 2123-2167

18. Miehe C., Schröder J., Bayreuther C., 2002b, On the homogenisation analysis of composite materials based on discretized fluctuations on the microstructure, *Acta Mechanica*, **155**, 1-16

19. Miehe C., Schröder J., Becker M., 2002c, Computational homogenization analysis in finite elasticity: material and structural instabilities on the micro- and macro-scales of periodic composites and their interaction, *Comp. Met. Appl. Mech. Eng.*, **191**, 4971-5005

20. Oden J.T., Zohdi T.I., 1997, Analysis and adaptive modeling of highly heterogeneous elastic structures, *Comp. Met. Appl. Mech. Eng.*, **148**, 367-391

21. Reuss A., 1929, Calculation of flow limits of mixed crystals on the basis of the plasticity of mono-crystals, *Z. Angew. Math. Mech.*, **9**, 49-58

22. Schröder J., 2000, *Homogenisierungsmethoden der nichtlinearen Kontinuumsmechanik unter Beachtung von Stabilitäts Problemen*, Habilitationsshrift, Universität Stuttgart

23. Simo J.C., Hughes T.J.R., 1997, *Computational Inelasticity*, Springer Verlag

24. Talbot D.R.S., Willis J.R., 1985, Variational principles for inhomogeneous non-linear media, *IMA-Journal of Applied Mathematics*, **35**, 39-54

25. VOIGT W., 1889, Über die Beziehung zwischen den beiden Elasticitätskonstanten isotroper Körper, *Ann. Phys.*, Leipzig, **38**, 3, 573-587

26. ZIENKIEWICZ O.C., TAYLOR R.L., 2000, *The Finite Element Method*, Butterworth-Heinemann

27. ZOHDI T.I., ODENJ.T., RODIN G.J., 1993, Hierarchical modeling of heterogeneous bodies, *Comp. Met. Appl. Mech. Eng.*, **138**, 273-298

28. ZOHDI T.I., WRIGGERS P., 1999, A domain decomposition method for bodies with heterogeneous microstructure based on the material regularization, *Int. J. Sol. Struct.*, **36**, 2507-2525

29. ZOHDI T.I., WRIGGERS P., 2005, *Introduction to Computational Micromechanics*, Springer Series in: *Lecture Notes in Applied and Computational Mechanics*, **20**

30. ZOHDI T.I., WRIGGERS P., HUET C., 2001, A method of substructuring large-scale computational micromechanical problems, *Comp. Met. Appl. Mech. Eng.*, **190**, 13, 5639-5656

Zastosowanie wieloskalowej MES do modelowania nieliniowych wieloskładnikowych materiałów

Streszczenie

Praca dotyczy modelowania materiałów kompozytowych, a w szczególności zastosowania wieloskalowej metody elementów skończonych do tego celu. Metoda ta jest kombinacją MES oraz teorii homogenizacji i opiera się na podziale zadania symulacji niejednorodnego ciała na dwa poziomy: modelowania właściwego tego ciała i modelowania reprezentatywnego elementu materiału próbki, którego analiza ma uzupełnić brakujące efektywne równanie konstytutywne materiału. Połączenie obydwu poziomów symulacji jest osiągalne po wprowadzeniu warunku homogenizacji Hilla, który narzuca równość mocy w skali makro z mocą mikroskalową uśrednioną objętościowo. Zaletą metody jest jej aplikacyjność do analizy materiałów o bardzo różnorodnej mikrostrukturze. Zilustrowano to w pracy na przykładzie badań efektywnego zachowania dwu- i trójskładnikowych kompozytów.

Manuscript received February 23, 2009; accepted for print March 13, 2009